Supporting Information for Aqueous geochemical and microbial variation across discrete depth intervals in a peridotite aquifer assessed using a packer system in the Samail Ophiolite, Oman

Daniel B. Nothaft[a,*], Alexis S. Templeton[a,*], Eric S. Boyd[b], Juerg M. Matter[c], Martin Stute[d,e], Amelia N. Paukert Vankeuren[f], The Oman Drilling Project Science Team

[a] *Department of Geological Sciences, University of Colorado, Boulder, CO, USA*
[b] *Department of Microbiology & Immunology, Montana State University, Bozeman, MT*
[c] *National Oceanography Centre, University of Southampton, Southampton, UK*
[d] *Barnard College, New York, NY, USA*
[e] *Lamont-Doherty Earth Observatory, Columbia University, Palisades, NY, USA*
[f] *California State University, Sacramento, Sacramento, CA, USA*

Contents

List of Tables

List of Figures

*Corresponding authors
Email addresses: daniel.nothaft@colorado.edu (Daniel B. Nothaft), alexis.templeton@colorado.edu (Alexis S. Templeton)

S1. Supplementary 16S rRNA gene sequencing

Two 1 L autoclaved glass bottles were filled with drill foam/fluid that had surfaced after subsurface circulation during drilling of BA1A in 2017. The drilling foam and fluid was filtered through 0.22 μm polycarbonate filters at Colorado School of Mines. The drill foam/fluid samples totaled 1.5 L in volume and were split into two replicates, resulting in 0.75 L of foam/fluid filtered for each replicate. Nucleic acids concentrated onto the filters were extracted, amplified, and sequenced as described by Kraus et al. (2018). The drill foam/fluid samples (Figure S8) show very little taxonomic overlap with the fluids samples with packers (Main Text Figure 5).

In addition, a cell size fractionation experiment was performed for biomass filtering of BA1A in 2018. The sequential in-line filter housings described in the main text correspond to the three white cylinders near the bottom of Figure S2. Main Text Figure 5 shows the results of sequencing 0.22 μm pore-diameter filters only. Results of sequencing filters of all pore diameters are reported in (Figure S7).

S2. Tables

Table S1: Mixing extents based on Si, after Leong et al. (2020).

Sample ID	$\sum$Si/ $\left[\mu\text{mol} \cdot \text{L}^{-1}\right]$	Mixing extent / [% of $Mg^{2+} - HCO_3^-$ water]
BA1A_2018_55-66	1.97×10^2	65
BA1A_2018_100-400	4.49×10^1	15
BA1A_2019_0-30	3.33×10^2	110[a]
BA1A_2019_41-65	1.56×10^2	51
BA1A_2019_108-132	2.13×10^1	7.0
BA1D_2019_45-75	8.51	2.8
BA1D_2019_102-132	5.88	1.9

[a]BA1A_2019_0-30 has a calculated mixing extent > 100 % we performed these calculations using the same $Mg^{2+} - HCO_3^-$ end member as Leong et al. (2020), which had a $c_{\sum \text{Si}}$ of 303 μmol $\cdot$ kg. This sample should be considered representative of a typical $Mg^{2+} - HCO_3^-$ water.

S3. Figures

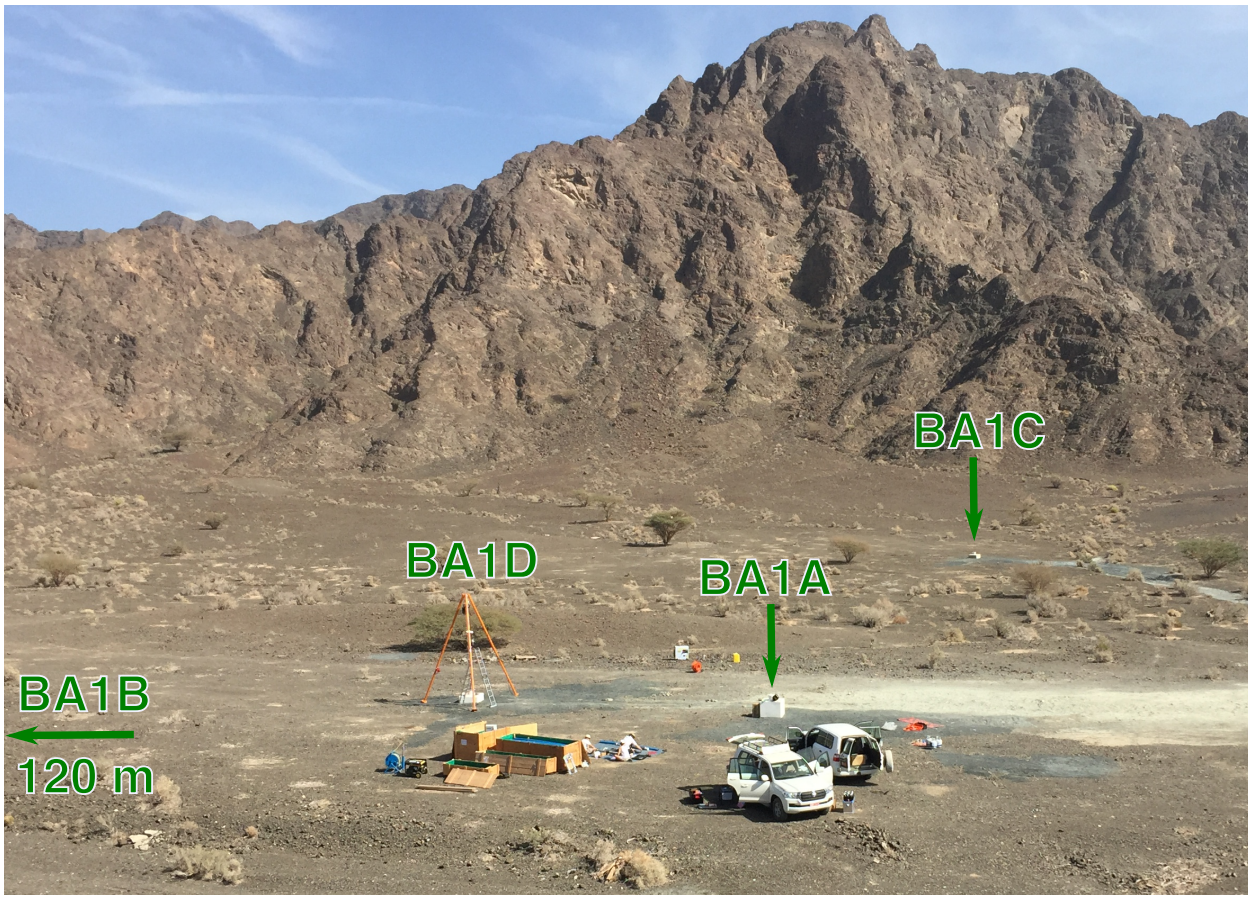

Figure S1: Packer installation at BA1D, January, 2019. The orange tripod, installed at BA1D in the photo, was used to suspend the packer assembly down hole. The wellhead of BA1A can be seen 15 m to the right of BA1D in the photo. The third rotary well at the BA1 site, BA1C, which collapsed shortly after drilling, is pictured in the background. The cored borehole, BA1B, is 120 m to the northwest, to the left of the frame.

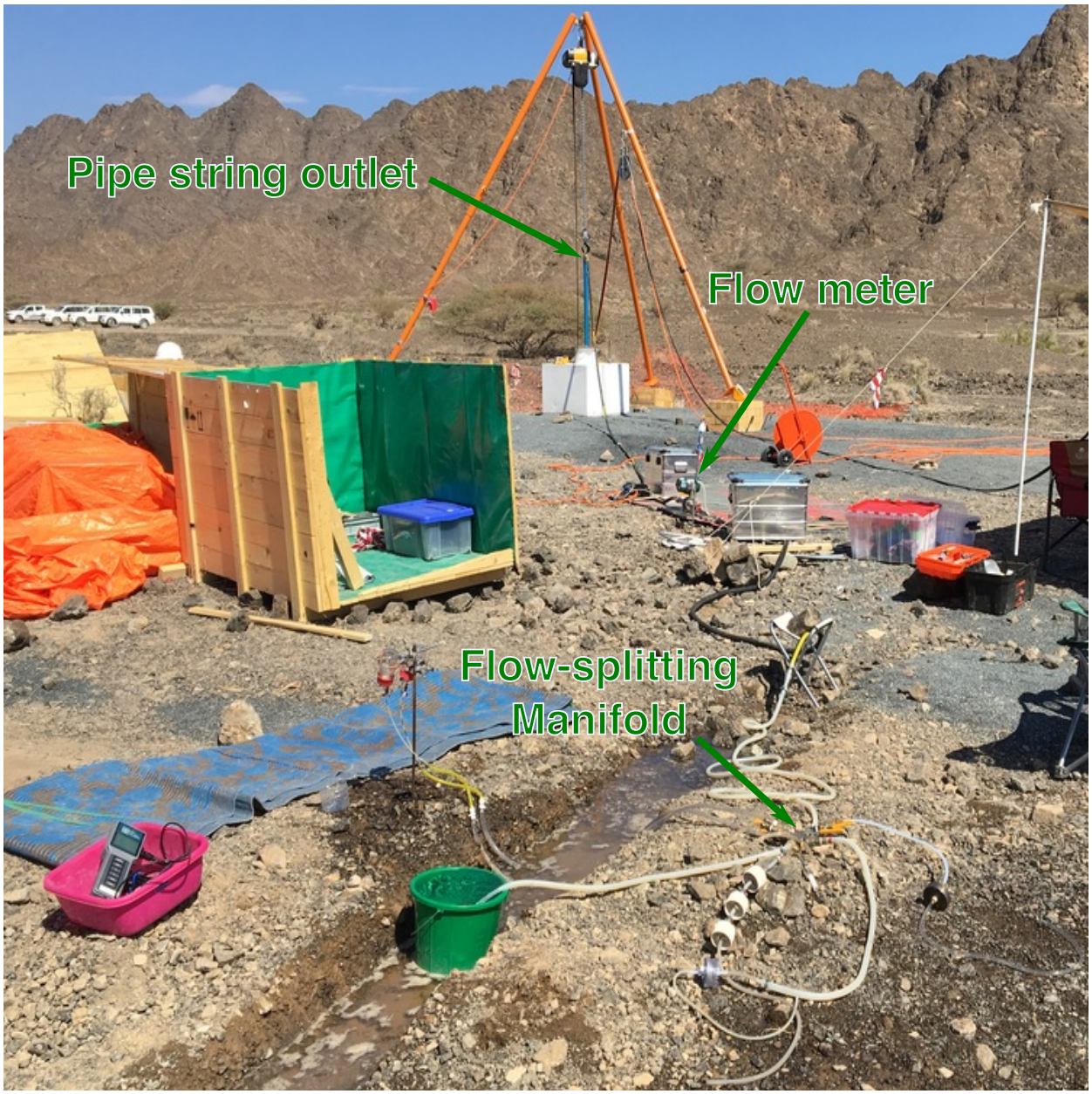

Figure S2: Fluid pumping and sampling at BA1A, February, 2019. Labeled arrows indicate the top of the pipe string, from which the pumped water flowed, the flow meter used for hydrologic pump tests, and the flow-splitting manifold used for fluid and biomass sampling.

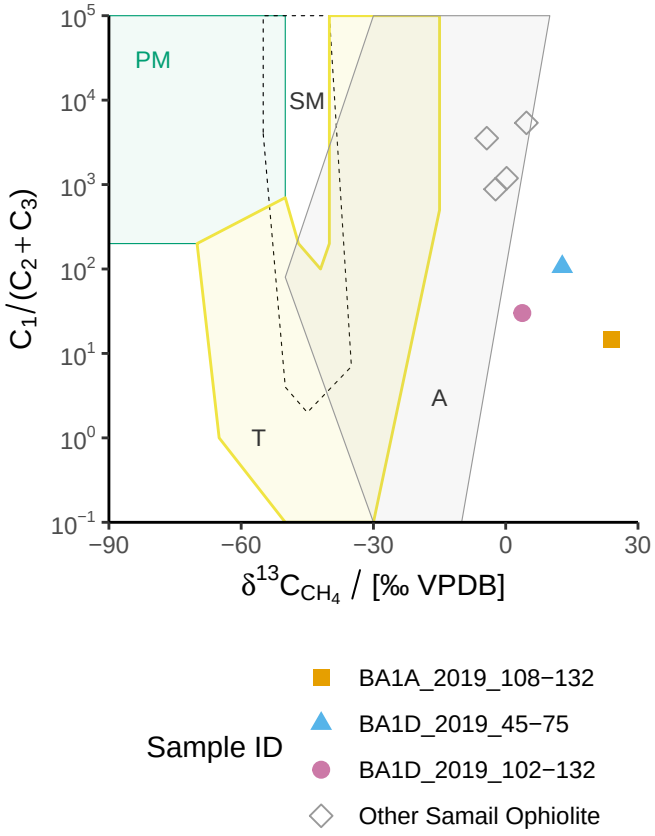

Figure S3: Plot of ratio of methane (C_1) to the sum of ethane (C_2) and propane (C_3) vs. $\delta^{13}C_{CH_4}$. Only analyses for which C_2 was above limit of quantitation are plotted. If C_3 was below limit of quantitation, its contribution to $C_1/(C_2+C_3)$ was assumed to be negligible, and therefore C_1/C_2 is plotted. Shaded fields of typical gas origin after Milkov and Etiope (2018). Contextual data from Samail Ophiolite from Nothaft et al., 2020; Etiope et al., 2015; Vacquand et al., 2018. *Abbreviations:* PM, primary microbial; SM, secondary microbial; T, thermogenic; A, abiotic.

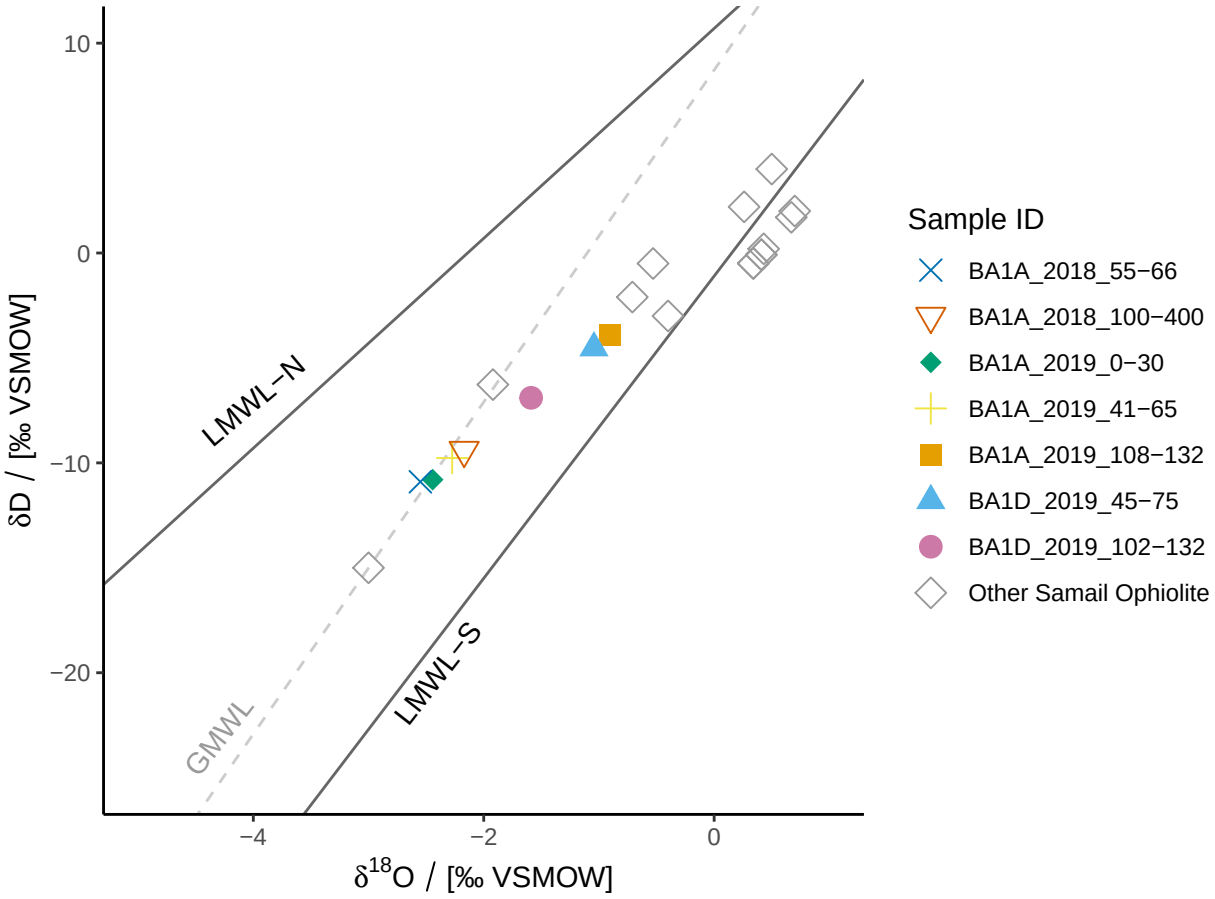

Figure S4: Plot of Oman groundwater stable isotopic compositions. Samples from 2012 were reported in Paukert Vankeuren et al. (2019). Samples from 2014 reported in Miller et al. (2016). Samples from 2018 (apart from BA1A) reported in Nothaft et al. (2020) *Abbreviations:* LMWL-N and LMWL-S, Oman local meteoric water lines derived from northern and southern sources, respectively (Weyhenmeyer et al., 2002); GMWL, global meteoric water line (Terzer et al., 2013).

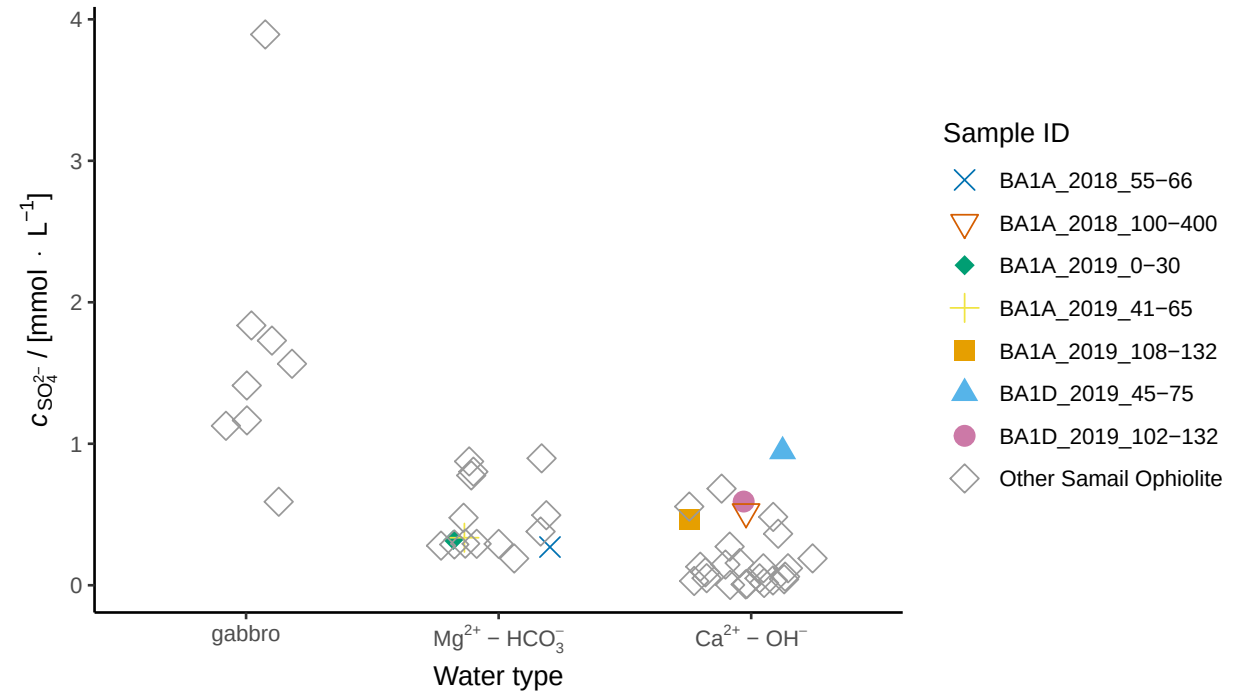

Figure S5: SO_4^{2-} concentrations in Samail Ophiolite wells. Data from Miller et al., 2016; Rempfert et al., 2017; Kraus et al., 2018; Nothaft et al., 2020.

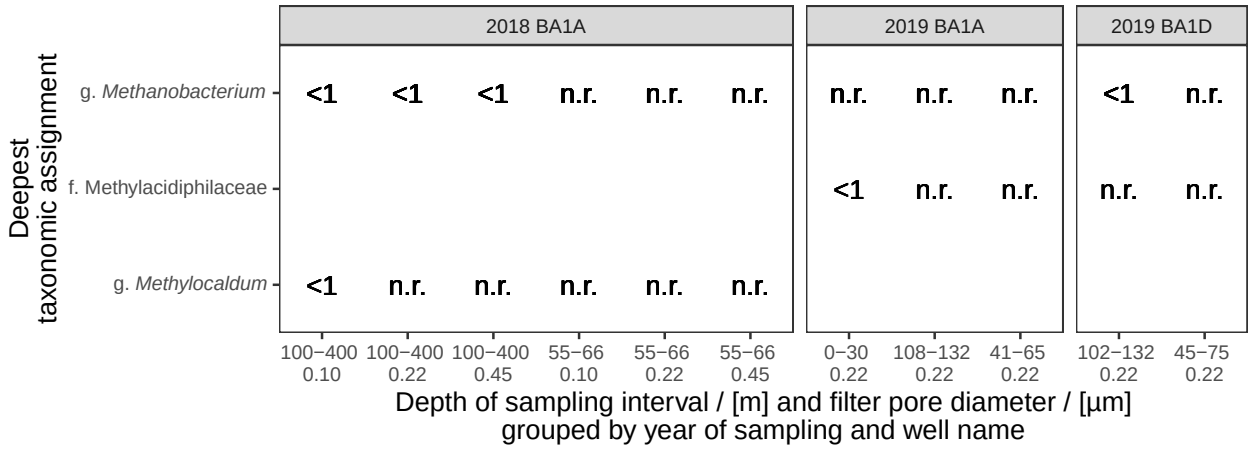

Figure S6: 16S rRNA gene read relative abundances of DNA extracted from filter-concentrated groundwaters from BA1A and BA1D affiliated with CH_4-cycling taxa. Read relative abundances are reported as percentages rounded to the ones place. Cases when a taxon was detected in a sample and was $< 1\,\%$ read relative abundance after rounding are labeled "< 1". Cases when no reads of a taxon were detected in a sample, but when that taxon was detected in 16S gene reads of other Oman samples obtained during the same sampling year, are labeled "n.r." Cases when no reads were detected in any Oman sample within the data set of a given year are blank."

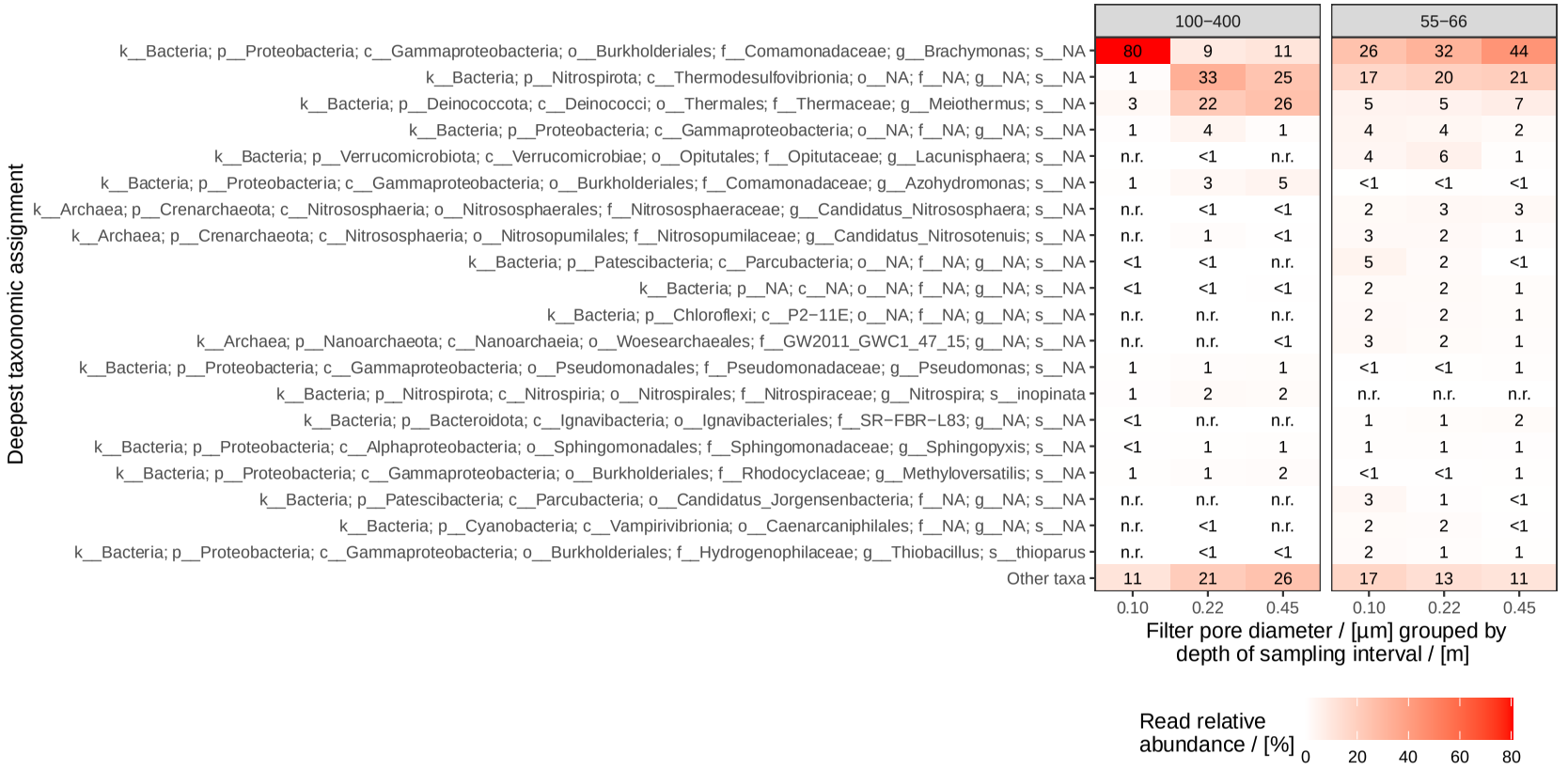

Figure S7: 16S rRNA gene read relative abundances of 20 most abundant taxonomic assignments in DNA extracted from groundwaters from which biomass was concentrated using inline filters of sequentially decreasing pore diameters from well BA1A in 2018. Read relative abundances are reported as percentages rounded to the ones place. Cases when a taxon was detected in a sample and was $< 1\,\%$ read relative abundance after rounding are labeled "< 1". Cases when no reads of a taxon were detected in a sample, but when that taxon was detected in 16S gene reads of other Oman samples obtained during the same sampling year, are labeled "n.r." Cases when no reads were detected in any Oman sample within the data set of a given year are blank."

Figure S8: 16S rRNA gene read relative abundances in of 20 most abundant taxonomic assignments in DNA and cDNA (from RNA) (Kraus et al., 2018) extracted from drill foam / fluid effluent from BA1A, acquired during drilling in 2017. Read relative abundances are reported as percentages rounded to the ones place. Cases when a taxon was detected in a sample and was $< 1\,\%$ read relative abundance after rounding are labeled "< 1". Cases when no reads of a taxon were detected in a sample, but when that taxon was detected in 16S gene reads of other Oman samples obtained during the same sampling year, are labeled "n.r." Cases when no reads were detected in any Oman sample within the data set of a given year are blank.

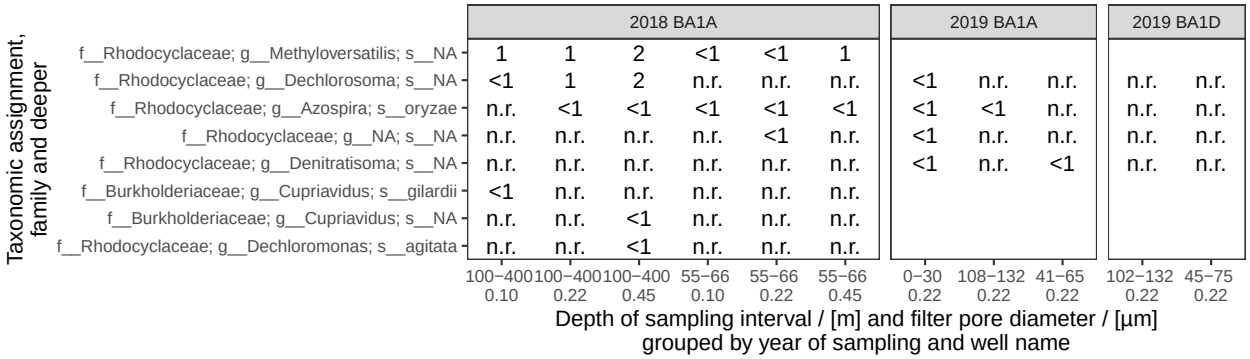

Figure S9: 16S rRNA gene read relative abundances of DNA extracted from filter-concentrated groundwaters from BA1A and BA1D affiliated with S-oxidizing taxa noted by Rempfert et al. (2017) (presented at family level and deeper). Read relative abundances are reported as percentages rounded to the ones place. Cases when a taxon was detected in a sample and was $< 1\,\%$ read relative abundance after rounding are labeled "< 1". Cases when no reads of a taxon were detected in a sample, but when that taxon was detected in 16S gene reads of other Oman samples obtained during the same sampling year, are labeled "n.r." Cases when no reads were detected in any Oman sample within the data set of a given year are blank."

S4. References

Etiope, G., Judas, J., Whiticar, M.. Occurrence of abiotic methane in the eastern United Arab Emirates ophiolite aquifer. Arabian J Geosci 2015;8(12):11345–11348. doi:10.1007/s12517-015-1975-4.

Kraus, E.A., Stamps, B.W., Rempfert, K.R., Nothaft, D.B., Boyd, E.S., Matter, J.M., Templeton, A.S., Spear, J.R.. Biological methane cycling in serpentinization-impacted fluids of the Samail ophiolite of Oman. AGU Fall Meeting Abstracts 2018;.

Leong, J., Howells, A., Robinson, K., Shock, E.. Diversity in the compositions of fluids hosted in continental serpentinizing systems. In: International Conference on Ophiolites and the Oceanic Lithosphere: Proceeding and Abstract Book. 2020. p. 130–131.

Milkov, A.V., Etiope, G.. Revised genetic diagrams for natural gases based on a global dataset of >20,000 samples. Org Geochem 2018;125:109–120. doi:10.1016/j.orggeochem.2018.09.002.

Miller, H.M., Matter, J.M., Kelemen, P., Ellison, E.T., Conrad, M.E., Fierer, N., Ruchala, T., Tominaga, M., Templeton, A.S.. Modern water/rock reactions in Oman hyperalkaline peridotite aquifers and implications for microbial habitability. Geochim Cosmochim Acta 2016;179:217 – 241. URL: http://www.sciencedirect.com/science/article/pii/S0016703716300205. doi:10.1016/j.gca.2016.01.033.

Nothaft, D.B., Templeton, A.S., Rhim, J.H., Wang, D.T., Labidi, J., Miller, H.M., Boyd, E.S., Matter, J.M., Ono, S., Young, E.D., Kopf, S.H., Kelemen, P.B., Conrad, M.E., The Oman Drilling Project Science Team, . Geochemical, biological and clumped isotopologue evidence for substantial microbial methane production under carbon limitation in serpentinites of the Samail Ophiolite, Oman. Earth and Space Sci Open Archive 2020;URL: https://doi.org/10.1002/essoar.10504124.1. doi:10.1002/essoar.10504124.1.

Paukert Vankeuren, A.N., Matter, J.M., Stute, M., Kelemen, P.B.. Multitracer determination of apparent groundwater ages in peridotite aquifers within the Samail ophiolite, Sultanate of Oman. Earth Planet Sci Lett 2019;516:37–48. doi:10.1016/j.epsl.2019.03.007.

Rempfert, K.R., Miller, H.M., Bompard, N., Nothaft, D., Matter, J.M., Kelemen, P., Fierer, N., Templeton, A.S.. Geological and geochemical controls on subsurface microbial life in the Samail Ophiolite, Oman. Front Microb 2017;8(56):1–21. doi:10.3389/fmicb.2017.00056.

70 Terzer, S., Wassenaar, L.I., Araguás-Araguás, L.J., Aggarwal, P.K.. Global isoscapes for δ^{18}O and δ^{2}H in precipitation:
71 improved prediction using regionalized climatic regression models. Hydrol Earth Syst Sci 2013;17(11):4713–4728. URL:
72 https://www.hydrol-earth-syst-sci.net/17/4713/2013/. doi:10.5194/hess-17-4713-2013.
73 Vacquand, C., Deville, E., Beaumont, V., Guyot, F., Sissmann, O., Pillot, D., Arcilla, C., Prinzhofer, A.. Reduced gas
74 seepages in ophiolitic complexes: evidences for multiple origins of the H_2-CH_4-N_2 gas mixtures. Geochim Cosmochim Acta
75 2018;223:437–461. doi:10.1016/j.gca.2017.12.018.
76 Weyhenmeyer, C.E., Burns, S.J., Waber, H.N., Macumber, P.G., Matter, A.. Isotope study of moisture sources, recharge
77 areas, and groundwater flow paths within the eastern Batinah coastal plain, Sultanate of Oman. Water Resources Research
78 2002;38(10). doi:10.1029/2000WR000149.